DOI: 10.1002/chem.200801076

The Effect of a Complexed Lithium Cation on a Norcarane-Based Radical Clock

Christof M. Jäger, Matthias Hennemann, and Timothy Clark*[a]

Abstract: Density-functional theory (DFT) and ab initio calculations have been used to investigate the effect of a complexed lithium cation on the radical-clock rearrangement of the 2-norcaranyl radical to the 3-cyclohexenylmethyl radical. As found earlier for ring-closing radical clocks, complexation with a metal ion leads to a significant lowering of the barrier to rearrangement. DFT calculations on a model for the norcaranyl clock in cytochrome P450 confirm the two-state reactivity proposal of Shaik et al. and indicate that the porphyrin exerts little or no electrostatic effect on the rearrangement barrier.

Keywords: ab initio calculations · density functional calculations · radical clocks · radicals · rearrangement

Introduction

Radical clocks[1] have commonly been used as a diagnostic tool for radical intermediates in unknown reaction mechanisms or for determining rate constants for radical reactions that compete with the "clock" rearrangement. In classical physical–organic mechanistic studies, they helped obtain a more distinct picture of the factors that govern radical reactivity.[2–9] However, as the radical reactions to be investigated became faster, as is the case for many biological reactions, the classical radical clocks based on the ring-closing addition of a radical center to a multiple bond to give a five-membered ring became too slow. A new generation of faster radical clocks based on the ring-opening of cyclopropylmethyl-type radicals was introduced.[6–9] Radical clocks have also been the subject of numerous theoretical studies that use both ab initio[10–13] and density-functional theory (DFT)[12,14–18] methods.

Radical clocks work by forming a radical intermediate that undergoes a known, fast unimolecular rearrangement to give characteristic products. These rearrangements usually belong to the two types outlined above. The radical rearrangement rate is assumed to be constant under all reaction conditions. However, for a ring-closure-type radical clock, we[19] were able to show that complexation of the double bond of the intermediate hex-1-en-6-yl radical[20] to a lithium cation decreases the calculated activation barrier for the ring-closing rearrangement significantly. This effect is supported indirectly by recent work of Michl and co-workers,[21,22] who showed that "naked" lithium cations have a catalyzing effect on the radical polymerization of terminal olefins, in accord with a proposal made 20 years ago on the basis of ab initio calculations[23] and a recent more-detailed study at higher theoretical levels.[24] However, all these observations pertain to radicals that contain a double bond, which can complex the lithium cation moderately well.[25] We have now extended our studies of electrostatic perturbations of the rates of radical-clock rearrangements to a cyclopropane-ring-opening clock, for which the initial intermediate does not contain a double bond to complex the metal cation.

Norcarane, bicyclo[4.1.0]heptane, is one mechanistic probe for the hydroxylation of alkanes by P450 enzymes that has been investigated by Newcomb et al.,[26] and Grooves and co-workers,[27] and others. These authors pointed out the ability of this probe to discriminate between radical and cationic intermediates. In contrast to results obtained earlier with other radical clocks, rearranged products derived from both reaction pathways were detected. The possible rearrangements of the norcaranyl radical are shown in Scheme 1.

[a] M. Sc. C. M. Jäger, Dr. M. Hennemann, Prof. T. Clark
Computer Chemie Centrum and Interdisciplinary Center for Molecular Materials
Friedrich-Alexander Universität Erlangen–Nürnberg Nägelsbachstrasse 25, 91052 Erlangen (Germany)
Fax: (+49) 9131-85-26565
E-mail: clark@chemie.uni-erlangen.de

Supporting information for this article is available on the WWW under http://dx.doi.org/10.1002/chem.200801076.

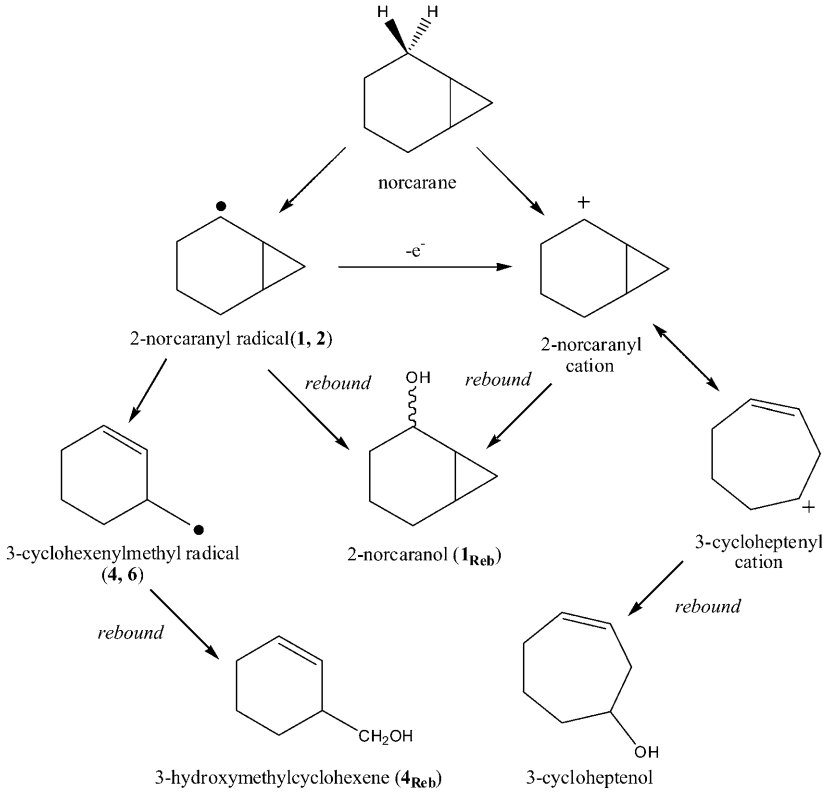

Scheme 1. Rearrangement pathways and products that result from the formation of either radical or cationic intermediates upon the oxidation of norcarane by P450 enzymes.

We recently reported a survey of unperturbed radical clock reactions calculated at the DFT and ab initio levels of theory that contained both radical-cyclization and ring-opening reactions, including the norcaranyl system.[28] We now demonstrate the effect of complexation of the norcaranyl radical to lithium cations and compare the results of this ring-opening reaction with the barrier-lowering effect for the cyclization of the hex-1-en-6-yl radical by lithium cation complexation.[19] We also discuss these results for the gas-phase reaction and present a comparison of these results with DFT calculations of the rearrangement in a model-enzyme active site with respect to their relevance for the mechanistic studies of the rearrangement mechanisms in cytochrome P450 enzymes.

Results and Discussion

The parent reaction: We recently reported the results of DFT and ab initio calculations for the unperturbed rearrangement of the 2-norcaranyl radical.[28] We found two low-energy conformations, namely, **1** and **2** (see scheme 1), for the initial radical with a CBS-RAD-calculated energy difference of 1.4 kcal mol^{-1}. We included CBS-RAD energies for comparison with our earlier work. However, we have also given energies calculated with the more recent CBS-QB3 procedure wherever possible (shown in brackets). Generally, the two techniques agree very well, and details of both are given in the Methods section.

The most stable conformation **1** rearranges to product **4** via transition state **3**‡, whereas the other conformer **2** rearranges to product **6** via transition state **5**‡. The calculated transition barriers at the CBS-RAD (and CBS-QB3) level of theory are 5.9 (6.0) and 7.3 (7.6) kcal mol^{-1} relative to conformer **1**, respectively.

As mentioned, a second rearrangement is possible in the norcaranyl system. The radical intermediate can undergo an electron transfer to give a cationic intermediate, which ring opens to give a seven-membered ring product. We calculated this rearrangement in the (inappropriate) radical oxidation state for both conformers to confirm that it is a pathway that applies exclusively to the cation oxidation state. Compound **1** rearranges to product **8** via transition state **7**‡ with an activation barrier of 10.7 (10.0) kcal mol^{-1} relative to **1**, and conformer **2** rearranges to **10** via **9**‡ with an activation barrier of 9.3 (9.1) kcal mol^{-1} relative to **1** and 7.9 (7.9) kcal mol^{-1} relative to **2**. Interestingly, the rearrangement barrier is lower for conformer **2**. However, neither rearrangement is competitive with the pathways that give **4** and **6**. Therefore, these rearrangements do not represent possible radical rearrangements.

The calculated relative energies are shown in Table 1 and the schematic energy diagram of the rearrangement is

Table 1. Calculated relative energies for the radical rearrangement of the 2-norcaranyl radical.

	B3LYP/6-31G(d)[a]	QCISD/6-31G(d)[a]	CBS-RAD (QCISD,-B3LYP)[a]	CBS-QB3[a]
1	0.0	0.0	0.0	0.0
2	1.1	1.0	1.4	1.2
3‡	7.4	10.0	5.9	6.0
4	−2.4	−3.2	−2.9	−2.7
5‡	8.8	11.6	7.3	7.6
6	−2.8	−3.5	−3.8	−3.0
7‡	11.3	14.5	10.7	10.0
8	−1.9	−1.4	−0.7	−0.8
9‡	10.4	13.3	9.3	9.1
10	−1.4	−1.5	−1.0	−0.9

[a] All the relative energies are given in kcal mol^{-1}; the absolute energies and $<S^2>$ values are given in the Supporting Information; the B3LYP/6-31G(d) and QCISD/6-31G(d) energy values are corrected with unscaled B3LYP/6-31-G(d) zero-point energies.

shown in Figure 1. Detailed energy tables, 3D representations of the structures, and important atom distances are available in the Supporting Information of our previous paper.[28]

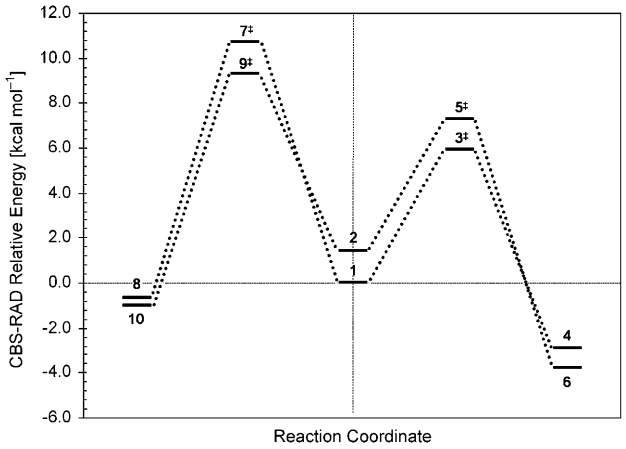

Figure 1. Schematic energy diagram of the rearrangements of the 2-norcaranyl radical.

2-Norcaranyl radical complexed to the Li^+ ion: We first investigated several possible positions for complexation of the lithium cation to the initial 2-norcaranyl radical. Figure 2 shows the four lowest energy complexes found in which the metal cation is complexed to the radical carbon C2 atom. Distances shorter than 2.5 Å to other carbon atoms are shown as dotted lines.

The most stable complex **1–Li** is derived from the more stable radical conformer **1** and shows close contact of the lithium ion to the carbon C1 and C7 atoms in addition to the complexation of the radical carbon C2 atom. A second, less stable complexation site is below the ring (**1b–Li**), with close contact between the lithium ion, the radical carbon C2 atom and C1 and C6. All the important interatomic distances are listed in the Supporting Information. The best estimate for the energy difference at the CBS-RAD (CBS-QB3) level is 1.7 (2.2) kcal mol^{-1} (see Table 2).

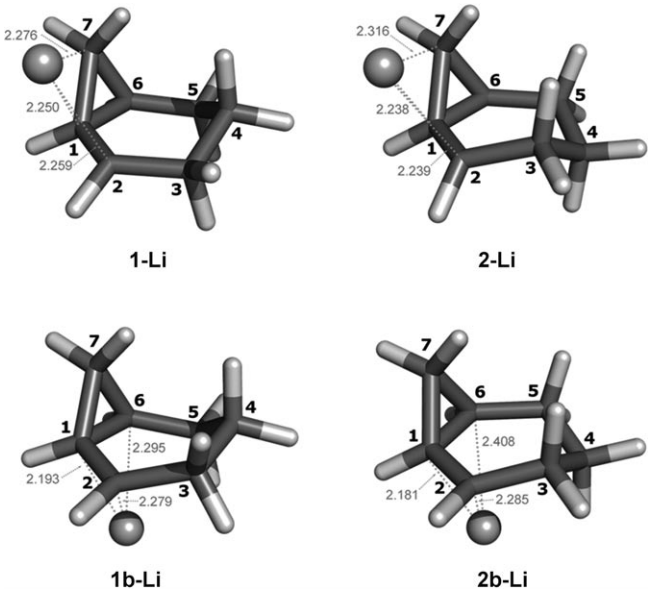

Figure 2. QCISD/6-31G(d) optimized structures of the 2-norcaranyl radical complexed to lithium cations.

Table 2. Calculated relative energies for the radical rearrangement of the lithium cation complexed to the 2-norcaranyl and 3-cyclohexenylmethyl radicals.

	B3LYP/ 6-31 G(d)[a]	QCISD/ 6–31 G(d)[a]	CBS-RAD (QCISD, B3LYP)[a]	CBS-QB3[a]
1–Li	0.0	0.0	0.0	0.0
1b–Li	2.7	2.7	1.7	2.2
2–Li	1.5	1.4	1.1	1.4
2b–Li	3.1	2.6	2.2	2.7
3‡–Li	4.6	6.6	4.0	4.6
3b‡–Li	10.0	12.2	9.4	9.2
4–Li	−4.1	−5.7	−1.7	−3.2
4b–Li	3.3	2.1	4.5	3.5
5‡–Li	6.6	8.8	6.3	6.8
5b‡–Li	10.3	12.7	10.3	10.1
6–Li	−3.5	−4.9	−1.3	−2.3
6b–Li	3.3	1.9	3.4	3.5

[a] All the relative energies are given in kcal mol^{-1}; the absolute energies and $<S^2>$ values are given in the Supporting Information; the B3LYP/6-31G(d) and QCISD/6-31G(d) energy values are corrected with unscaled B3LYP/6–31-G(d) zero-point energies.

The conformers labeled **2** are the next highest in energy and show the same modes of complexation as **1–Li** and **1b–Li** but to conformer **2** of the 2-norcaranyl radical. The energies relative to **1–Li** are 1.1 (1.4) and 2.2 (2.7) kcal mol^{-1} for **2–Li** and **2b–Li**, respectively. The CBS-RAD-calculated complexation energies between the lithium cation and the 2-norcaranyl radical are −34.4 and −34.6 kcal mol^{-1} for **1–Li** and **2–Li**, respectively, and are slightly lower for **1b–Li** and **2b–Li** (−32.7 and −33.5 kcal mol^{-1}, respectively).

The two different complexation modes lead to characteristic changes in the geometry of the organic moiety relative to the unperturbed radicals. In the case of **1–Li** and **2–Li**, in which the lithium ion is complexed above the ring, the C–C bond between atoms C1 and C7 is lengthened by 0.05 and 0.04 Å, respectively, and is therefore weakened. For the complexation from below the ring, the C–C bond between C1 and C6 is lengthened by 0.05 Å in both **1b–Li** and **2b–Li**.

Complexation of the Li^+ ion in the gas-phase reaction: The radical rearrangement pathways that lead to the 3-cyclohexenylmethyl radical product were calculated for all four precursor complexes. All the relative energies are listed in Table 2. The schematic energy diagram is shown in Figure 3. The first conformer **1–Li** rearranges to structure **4–Li** via the transition-state structure **3‡–Li**. The CBS-RAD (CBS-QB3)-calculated activation barrier is 4.0 (4.6) kcal mol^{-1}, and **3‡–Li** is the lowest energy transition state found. The

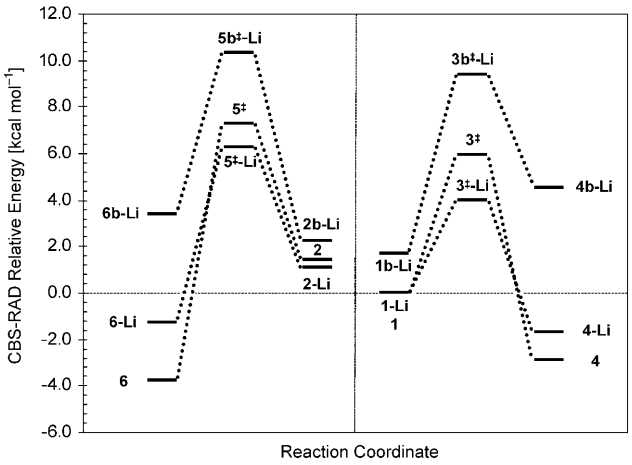

Figure 3. Schematic energy diagram of the radical rearrangement of the lithium-cation-complexed 2-norcaranyl radical to the 3-cyclohexenylmethyl radical relative to the unperturbed rearrangement.

rearrangement of the second conformer **2–Li** to product **6–Li** via the transition state **5**$^{+}$**–Li** is calculated to be less favorable with an energy barrier of 6.3 (6.8) kcal mol^{-1} relative to **1–Li** and 5.2 (5.4) kcal mol^{-1} relative to **2–Li**. However, both rearrangements are lower in energy relative to the unperturbed rearrangement. The lowest energy pathway shows a decrease of the activation barrier from 5.9 to 4.0 (4.6) kcal mol^{-1}.

The CBS-RAD complexation energies between the lithium cation and the radical species are −36.2 (**3**$^{+}$**–Li**), −33.3 (**4–Li**), −35.4 (**5**$^{+}$**–Li**), and −32.0 kcal mol^{-1} (**6–Li**). Thus, the lithium cation complexes most strongly to the transition state **3**$^{+}$**–Li** and slightly less strongly to **5**$^{+}$**–Li**. Note that the presence of odd electron bonds in the transition states suggests that they should complex better to cations than the minima,[29] as found for this example.

The geometrical changes relative to the unperturbed rearrangement are relatively small. The most significant changes are a slightly lengthened double bond (C1−C2) of products **4–Li** and **6–Li** (by 0.02 Å) and a slightly enlarged distance for the breaking bond between C1 and C7 in the transition states (0.03 and 0.02 Å for **3–Li** and **4–Li**, respectively).

The calculations show increased activation barriers for the rearrangement of the 2-norcaranyl radical complexed by lithium ions from below the ring. Complex **1b–Li** rearranges to **4b–Li** via the transition state **3b**$^{+}$**–Li** with a barrier of 9.4 (9.2) kcal mol^{-1} relative to **1–Li** and 7.7 (7.0) kcal mol^{-1} relative to **1b–Li**, whereas **2b–Li** rearranges to **6b–Li** via **5b**$^{+}$**–Li** with a barrier of 10.3 (10.1) kcal mol^{-1} relative to **1–Li** and 8.1 (7.4) kcal mol^{-1} relative to **2b–Li**.

The CBS-RAD complexation energies between the lithium cation and the radical decrease along the reaction pathway for both rearrangements. The values are −32.7 (**1b–Li**), −33.5 (**2b–Li**), −30.9 (**3b**$^{+}$**–Li**), −27.0 (**4b–Li**), −31.5 (**5b**$^{+}$**–Li**), and −27.2 kcal mol^{-1} (**6b–Li**). Thus, in this case the transition states **3b**$^{+}$**–Li** and **5b**$^{+}$**–Li** are less strongly complexed than expected, possibly because the radical center (and hence the unpaired electron density) lies on the opposite side of the ring to the site of complexation. During the rearrangement, the lithium cation looses its close contact with C6, as can be seen clearly in Figure 4. Moreover, the lithium cation is not complexed to the radical center in the products, which is caused by the relocation of the radical center from C2 to C7. In effect, the lithium cation can only complex the double bond of the product structure from below the ring. The double bonds of the products **4b–Li** and **6b–Li** are

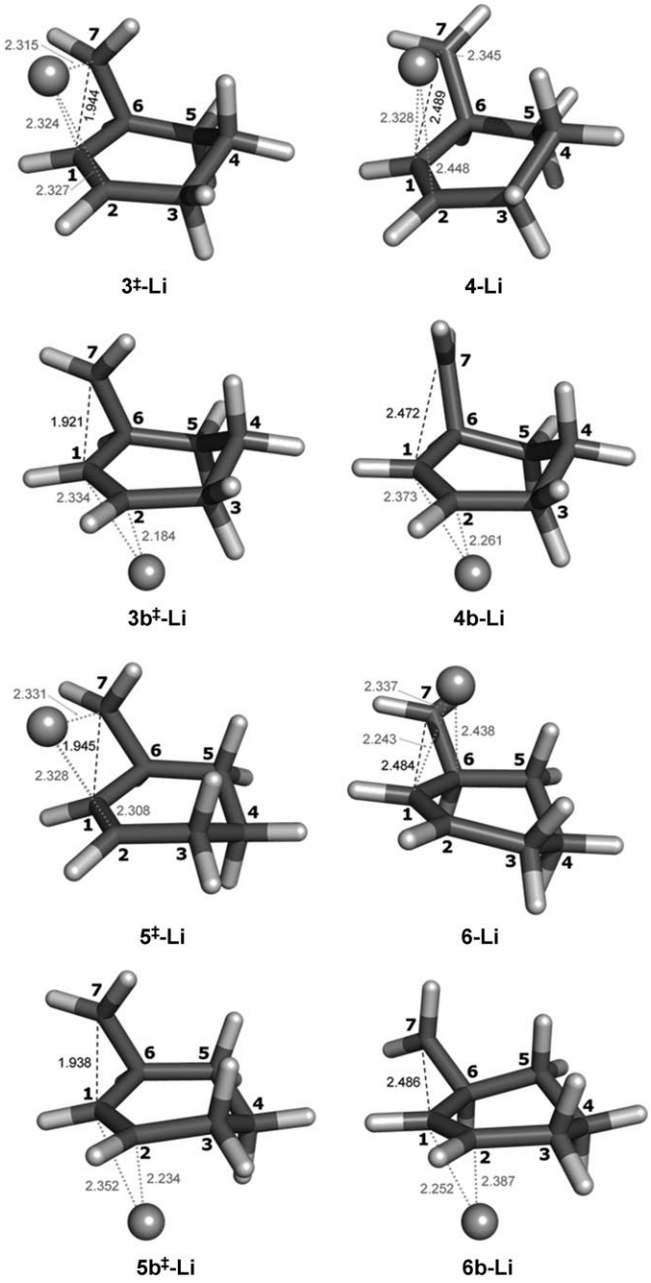

Figure 4. QCISD/6-31G(d) optimized structures of the rearrangement to the 1-cyclohexenylmethyl radical complexed to a lithium cation. For clarity, the atom numbers correspond to the IUPAC numbering of the initial radical. Therefore, they are not the correct IUPAC numbers for the 3-cyclohexenyl radical.

again lengthened by 0.02 Å relative to the unperturbed rearrangement.

Thus, as expected, the barrier for the rearrangement of both conformers of norcarane is lowered by the complexation of lithium cations from above the ring. However, the barriers are increased by the complexation of lithium cations from below the ring. This effect highlights the contrast between direct (odd-electron bonding) complexation to the radical center and Lewis acid–base complexation to the double bond. Only the former can be expected to provide electrostatic catalysis of the rearrangement. Moreover, the low-energy pathway of the unperturbed reaction **1** to **4** via $\mathbf{3}^{\ddagger}$ remains lowest in energy after complexation by the cation.

Nevertheless, it is also interesting to study the effect of the complexation of lithium cations on the radical rearrangement to the 3-cycloheptenyl radical product. We know from the unperturbed rearrangements that such a rearrangement is unlikely and has a high calculated activation barrier, whereby the rearrangement of the lowest energy conformer **1** is even more unlikely than that of conformer **2**. Again, we calculated possible rearrangement pathways for all complexation modes. We showed above that complexation from above the norcarane ring weakens the bond between C1 and C7, whereas complexation from below weakens the bond between C1 and C6. Thus, we only expect an energy-lowering effect for the ring opening between C1 and C6 on complexation from below the ring. However, for the sake of completeness we also investigated the rearrangements starting from **1–Li** and **2–Li**. The rearrangement of **1–Li** to **8–Li** via the transition state $\mathbf{7}^{\ddagger}$**–Li** is calculated to have an activation barrier of 12.9 (12.0) kcal mol^{-1}, which is 2.2 (2.0) kcal mol^{-1} higher than in the unperturbed reaction. Moreover, **8–Li** is a metastable intermediate that rearranges to **8c–Li** via transition state $\mathbf{7c}^{\ddagger}$**–Li** with an activation energy of only 1.2 (0.8) kcal mol^{-1} relative to **8–Li**. The relative energies are shown in Table 3, and the schematic energy diagram and the structures are shown in Figure 5 and Figure 6.

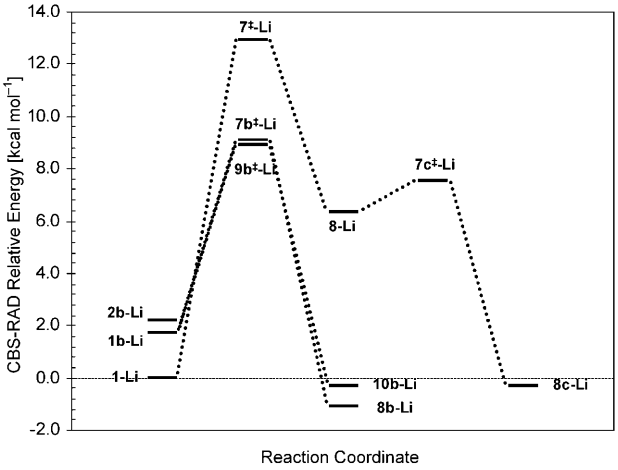

Figure 5. Schematic energy diagram of the rearrangement of the 2-norcaranyl radical to the 3-cycloheptenyl radical complexed to a lithium cation.

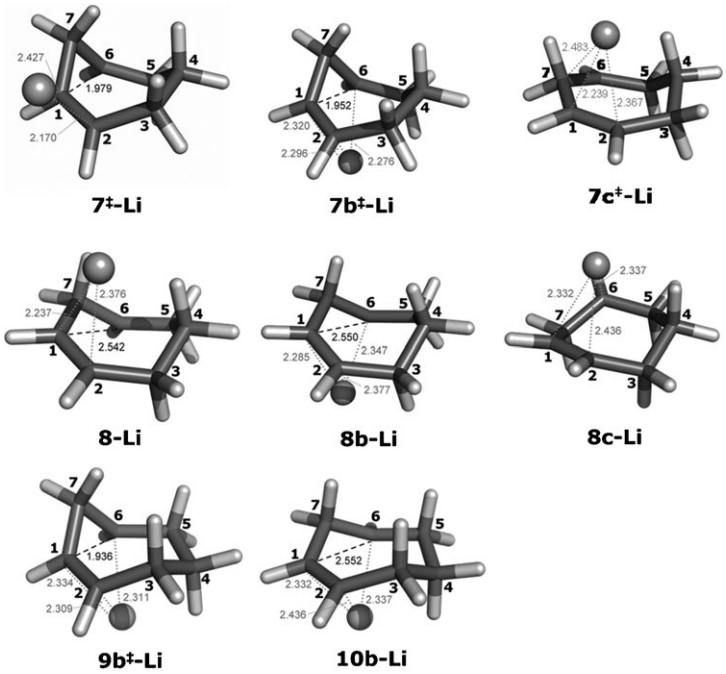

Figure 6. QCISD/6-31G(d) optimized structures for the rearrangement to the 3-cycloheptenyl radical complexed to a lithium cation. For clarity, the atom numbers correspond to the IUPAC numbering of the initial radical. Therefore, they are not the correct IUPAC numbers for the product.

Table 3. Calculated relative energies for the lithium-cation-complexed radical rearrangement to the cycloheptenyl product **10**.

	B3LYP/ 6–31 G(d)[a]	QCISD/ 6–31 G(d)[a]	CBS-RAD (QCISD, B3LYP)[a]	CBS-QB3[a]
$\mathbf{7}^{\ddagger}$**–Li**	11.0	14.7	12.9	12.0
$\mathbf{7b}^{\ddagger}$**–Li**	8.2	10.8	9.1	7.9
$\mathbf{7c}^{\ddagger}$**–Li**	3.5	4.6	7.5	5.5
8–Li	2.9	2.9	6.3	4.7
8b–Li	−4.3	−4.6	−1.1	−2.2
8c–Li	−3.9	−3.9	−0.3	−1.3
$\mathbf{9b}^{\ddagger}$**–Li**	8.3	10.7	8.9	8.1
10–Li	−4.3	−4.6	−1.1	−2.2
10b–Li	−3.9	−3.8	−0.3	−1.3

[a] All the relative energies are given in kcal mol^{-1}; the absolute energies and $<S^2>$ values are given in the Supporting Information; the B3LYP/6-31G(d) and QCISD/6-31G(d) energy values are corrected with unscaled B3LYP/6-31-G(d) zero-point energies.

The CBS-RAD complexation energies are −32.2 and −37.6 kcal mol^{-1} for $\mathbf{7}^{\ddagger}$**–Li** and $\mathbf{7c}^{\ddagger}$**–Li**, respectively, and −27.4 and −33.9 kcal mol^{-1} for **8–Li** and **8c–Li**, respectively. Therefore, the lithium cation complexes most strongly to the second transition state $\mathbf{7c}^{\ddagger}$**–Li** and least strongly to the intermediate structure **8–Li**. These energies correspond well to the changes in the complexation pattern of the lithium cation during the rearrangement. The first transition state $\mathbf{7}^{\ddagger}$**–Li** shows the loss of the close contact of the Li^+ ion to C7, which is still present in the intermediate **8–Li**. To form a more stable complex, the conformation of the radical

changes during the second rearrangement step coupled to a recomplexation of C7 in the transition state **7c^{+}–Li** to give the final structure **8c–Li**, in which the lithium cation shows close contacts to the newly formed double bond C1=C2 and the radical carbon C6 atom. The bond-opening distance between C1 and C6 in transition-state **7^{+}–Li** is 0.05 Å longer than in the unperturbed rearrangement. We were unable to find a rearrangement path to the cycloheptenyl product **10–Li** for the second conformer **2–Li**.

The "cation-like" rearrangements of **1b–Li** and **2b–Li** have calculated activation barriers of 9.1 (7.9) and 8.9 (8.1) kcal mol^{-1}, respectively, relative to **1–Li**. Thus, only a moderate barrier-lowering effect could be detected relative to the global minimum complex structure **1–Li**. However, the complexation of lithium cations shows an energy-lowering effect relative to the precursors **1b–Li** and **2b–Li**. In the case of the rearrangement of **1b–Li** to **8b–Li** via the transition state **7b^{+}–Li**, the barrier is lowered from 10.7 (10.0) to 7.4 (5.7) kcal mol^{-1} and in the case of the rearrangement of **2b–Li** to **10b–Li** via **9b^{+}–Li** from 7.8 (6.7) (relative to **2–Li**) to 6.7 (5.4) kcal mol^{-1}. Analogously to the unperturbed rearrangement, the barrier is lower for the less-stable conformer of norcarane. Unusually, the CBS-QB3 method predicts a larger barrier-lowering effect for the "cation-like" rearrangement than the CBS-RAD calculations. The CBS-RAD complexation energies are −36.0, −34.8, −34.9, and −34.5 kcal mol^{-1} for **7b–Li**–**10b–Li**, respectively. Therefore, the lithium ion complexes to the transition structure **7b^{+}–Li** best.

In both transition states and both products, the lithium cation shows close contacts to C1, C2, and C6. Moreover, the resulting structure **10b–Li** (derived from the rearrangement of **1b–Li**) is enantiomeric to the conformationally rearranged structure **8c–Li**, which is derived from complex **1–Li** rather than **2–Li**. Thus, the second rearrangement step found for the complexation from above the ring in which the conformation of C7 changes can also be seen as a change of the complexation of the lithium cation to give the more stable radical conformation with the lithium cation complexed from below the ring. This effect might also explain why we were unable to find a direct rearrangement pathway from the second conformer **2–Li** to give the product **10–Li**, which is enantiomeric to **8b–Li**.

Models for oxidation by cytochrome P450: Experimental studies[26,27] of the hydroxylation of norcarane by cytochrome P450 enzymes have shown that products from both the radical and cationic rearrangement pathways could be detected in small amounts. However, it is still not clear whether the "cationic" products arise from a cationic intermediate formed by electron transfer after the formation of the radical intermediate, beforehand, or both. To understand the possible reaction pathways for P450-mediated alkane hydroxylation, Shaik and co-workers[30] performed several theoretical studies on reactions that have been characterized experimentally. The authors found support for the two-state reaction (TSR) mechanism that they originally reported as a low-energy rebound pathway for the hydroxylation of methane.[31]

The novel feature of the TSR mechanism is that the product distribution of the hydroxylation of an alkane results from a complex interplay between two reactive states of the active ferryl–oxene–porphyrine complex (compound 1)[32] at the active site of the enzyme. Shaik and co-workers[31] calculated transition structures, intermediates, and products for the low-spin (doublet) and high-spin (quartet) states and found significant differences between the two spin states. In the initial bond-activating H-abstraction step, a hydrogen atom is transferred from the alkane to compound 1 to form an alkyl radical complexed to the iron–hydroxo complex. This step is followed directly by the rebound of the hydroxy group. For the low-spin complex, the rebound is almost barrierless, whereas the high-spin complex forms a radical that has a significant barrier for rebound. It is therefore possible that the discrete radical formed in the high-spin reaction path can undergo a rearrangement to result in a new hydroxylation product.

In recent years, further theoretical investigations of C–H hydroxylation by cytochrome P450 enzymes have been reported.[33–37] Currently, ten cases have been studied exhaustively.[34,35] Both DFT and hybrid QM/MM[36,37] calculations have been used to shed light on the complexity of the different electronic states that appear during the catalytic cycle of compound I during the oxidation of different organic compounds. This work has allowed the picture of the TSR mechanism of compound 1 to be expanded to one of multistate reactivity (MSR) for some cases, such as C=C epoxidation.[35]

We now use the results of our DFT calculations on norcarane to study the rearrangement of norcarane in a model-active site. The goal of these calculations was to determine whether the iron–hydroxo complex can also exert an electrostatic effect on the barrier to the rearrangement of the radical. If this were the case, conclusions drawn from radical-clock studies on the reactions of cytochrome P450 enzymes would have to be questioned. The results described above for the two conformers and especially the effects of the complexation of the lithium cation from the two sides of the ring structure help to indicate reasonable positions for norcarane relative to the iron–oxo–porphyrin complex. As we are principally interested in whether the electrostatic effect of the porhyrin can be significant, we have used a simple truncated active-site model, rather than trying to reproduce the behavior of the enzyme more completely by using QM/MM studies.

We used the Dmol^{3} module[38] of the Accelrys Materials Studio software package[39] for these calculations. Transition states, intermediates, and products were located by a linear synchronous transit/Quadratic synchronous transit (LST/QST) transition-state search,[40] nudged elastic-band transition-state confirmation,[41] and geometry-optimization calculations. We investigated the radical rearrangement behavior of conformer **1**, which is part of the low-energy rearrangement pathway to give radical **4** in the gas-phase calculations.

We focused on the rearrangement of the radical and the radical rebound to determine whether the rearrangement or direct rebound is favored.

Table 4 shows the relative energies for the radical rearrangement during the hydroxylation of norcarane for the low- and high-spin states derived from transition-state search calculations. Figure 7 and Figure 8 show the geometries and important atom distances for the rearrangement and the rebound.

Table 4. Calculated relative energies for the rearrangement and rebound of norcarane bound to the modeled enzyme site.

Relative energy [kcal mol^{-1}][a]		Relative energy [kcal mol^{-1}][a]	
$^{2}\mathbf{1}$	0.0	$^{4}\mathbf{1}$	0.0
$^{2}\mathbf{3}^{\ddagger}$	7.0	$^{4}\mathbf{3}^{\ddagger}$	8.5
$^{2}\mathbf{4}$	−2.5	$^{4}\mathbf{4}$	0.6
$^{2}\mathbf{1}^{\ddagger}_{\mathbf{Reb}}$	0.3	$^{4}\mathbf{1}^{\ddagger}_{\mathbf{Reb}}$	14.4
$^{2}\mathbf{1}_{\mathbf{Reb}}$	−55.9	$^{4}\mathbf{1}_{\mathbf{Reb}}$	−30.7
		$^{4}\mathbf{4}^{\ddagger}_{\mathbf{Reb}}$	10.0
		$^{4}\mathbf{4}_{\mathbf{Reb}}$	−37.4

[a] Derived from the LST/QST transition-state search calculations.

In the low-spin pathway, the rebound of the radical intermediate $^{2}\mathbf{1}$ occurs almost without a barrier to give the alcohol $^{2}\mathbf{1}_{\mathbf{Reb}}$ with a relative energy of −55.9 kcal mol^{-1}. The alternative rearrangement of the radical to $^{2}\mathbf{4}$ has a calculated barrier of 7.0 kcal mol^{-1} relative to $^{2}\mathbf{1}$ and is therefore not competitive.

The reaction profile of the high-spin state differs significantly from its low-spin equivalent. The direct-rebound process has a pronounced barrier via $^{4}\mathbf{1}^{\ddagger}_{\mathbf{Reb}}$, which is 14.4 kcal mol^{-1} higher in energy than $^{4}\mathbf{1}$. The barrier for the rearrangement of the 2-norcaranyl radical ($^{4}\mathbf{3}^{\ddagger}$) to the 3-cyclohexenyl radical complex $^{4}\mathbf{4}$ is 5.9 kcal mol^{-1} lower than this rebound barrier. The rearrangement barrier calculated at the same level of theory for the unperturbed norcaranyl radical of 8.7 kcal mol^{-1} is almost identical to this barrier (8.5 kcal mol^{-1}). The subsequent rebound of the rearranged radical $^{4}\mathbf{4}$ has a barrier ($^{4}\mathbf{4}^{\ddagger}_{\mathbf{Reb}}$) of 10.0 kcal mol^{-1} relative to $^{4}\mathbf{4}$ to give the product complex $^{4}\mathbf{4}_{\mathbf{Reb}}$. The schematic reaction pathway shown in Figure 9 indicates that the rebound pathway with rearrangement of the radical is lower in energy than the direct rebound.

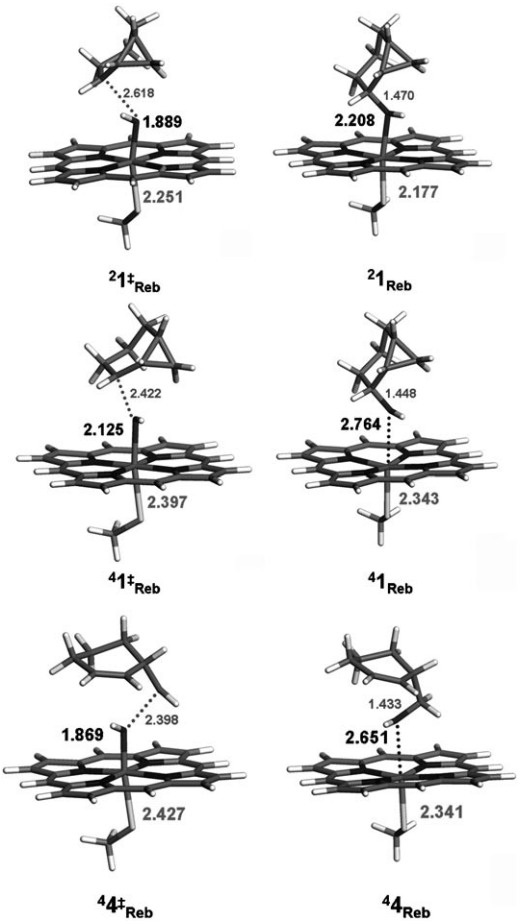

Figure 8. Structures of the rebound of unrearranged and rearranged norcarane.

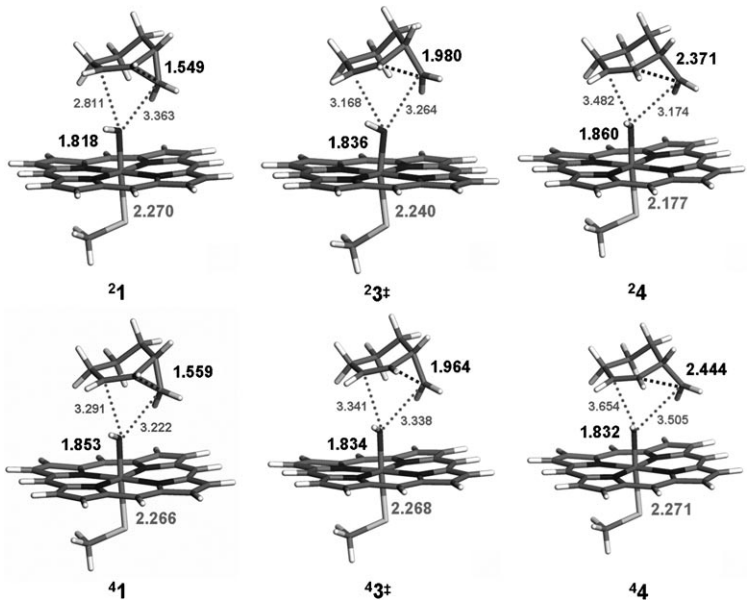

Figure 7. Structures of the rearrangement of norcarane bound to the low- and high-spin species.

Conclusion

The gas-phase calculations for the radical rearrangement of the 2-norcaranyl radical show

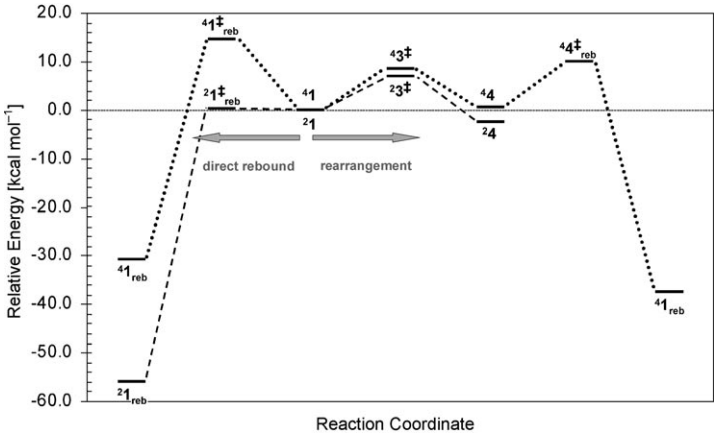

Figure 9. Schematic energy diagram of the rearrangement and rebound pathways of the 2-norcaranyl radical bound to the high-spin state.

that complexation of the radical to a lithium cation lowers the barrier to rearrangement in analogy to our previous work.[19] It is not obvious that this effect, which was studied previously for a ring-closing clock, should also apply to a ring-opening reaction. In the case of the cyclization of the hex-1-en-6-yl radical, the lithium cation showed high preference toward complexing the double bond of the radical.[19] In the 2-norcaranyl rearrangement, the double bond is formed during the reaction and the complexation patterns therefore differ.

It is important that the radical carbon atom is complexed by the lithium cation in the initial and rearranged radical structures for the barrier to be lowered. Complexation of the double bond of the rearranged product alone is not sufficient. Moreover, it is important to highlight the complexation of the bonds of the cyclopropane ring. As mentioned above, the complexed bond is weakened, which favors cleavage of this bond. This effect is enhanced by the strong donor character of the cyclopropane ring bonds.

Therefore, the energy-lowering effect of the radical rearrangement to the cyclohexenylmethyl radical appears only when the lithium cation complexes 2-norcaranyl from the top (radical) side of the ring structure. Complexation from the opposite side only lowers the barriers for the hypothetical alternative radical rearrangement to the cycloheptenyl radical. In reality, this rearrangement is believed to be observed after electron transfer to form a cationic intermediate. Our calculations do not suggest that this rearrangement could result from a Li^+-catalyzed radical rearrangement.

The results for the cytochrome P450 model correspond well to the two-state rebound mechanism of Shaik and coworkers.[31] We could show that the rearrangement of the 2-norcaranyl to 3-cyclohexyl radical is likely in the high-spin state. Therefore, the amount of rearranged product should depend strongly on the proportion of high-spin species in the reaction. Our calculations are not reliable enough to be able to predict the relative stabilities of the high- and low-spin states along the reaction pathways, so we cannot make any quantitative predictions of the yields of the individual products.

We note that complexation with the cytochrome P450 model does not affect the calculated barrier to the radical rearrangement at all, in contrast to complexation with the lithium cation. It is not unreasonable to postulate such an effect because electrostatic catalysis should be largely independent of whether the perturbing charge is positive or negative.[29] However, the OH group in the iron–hydroxy species is relatively nonpolar, with natural bond orbital (NBO) charges of only −0.156 and −0.154 on the hydroxy groups in the low- and high-spin states, respectively. Their electrostatic effect can therefore be expected to be small.

Note that our calculations did not include the steric effect of the enzyme pocket, so we cannot say anything about the steric effect on possible radical rearrangements. This study does, however, help rule out a significant electrostatic catalysis or retardation of radical-clock rearrangements in cytochrome P450 reactions.

Methods

We used the Gaussian suite of programs[42] for the calculations of norcarane and norcarane complexed to lithium ions in the gas phase. The B3LYP[43] hybrid density functional and the 6–31G(d) basis set[44] were used to calculate initial geometry optimizations. Minima and transition states were confirmed as such by calculating their normal vibrations at this level of theory. The zero-point energies derived from these calculations were used for CBS-RAD (QCISD, B3LYP) calculations.[14–15] To obtain the CBS-RAD energies, further QCISD[45]/6-31G(d) geometry optimizations and CCSD(t)[46] single-point energy calculations were performed on all systems according to the procedure outlined by Radom and co-workers.[16] Additionally, CBS-QB3[47,48] calculations were performed on the QCISD[45]/6–31G(d) geometry optimized structures for all systems.

The Dmol^3 module[38] of the Accelrys Materials Studio software package[39] was used for the calculations of norcarane complexed to a model enzyme site. Transition-state confirmation and geometry optimization calculations, the gradient corrected potential PW91,[49] and the numerical DND basis set[41] were used for all the transition-state searches.

The active site was modeled by an iron–oxo–porphyrin complex model of the so-called compound **I**.[50]

Acknowledgements

We thank the Deutsche Forschungsgemeinschaft for financial support as part of grants Cl85/16-1 and Cl85/16-2. This work was also supported by the Interdisciplinary Center for Molecular Materials (ICMM).

[1] D. Griller, K. U. Ingold, *Acc. Chem. Res.* **1980**, *13*, 317–323.
[2] A. J. Castellino, T. C. Bruice, *J. Am. Chem. Soc.* **1988**, *110*, 7512–7519.

[3] R. Vanni, S. J. Garden, J. T. Banks, K. U. Ingold, *Tetrahedron Lett.* **1995**, *36*, 7999–8002.
[4] M. Newcomb, *Tetrahedron* **1993**, *49*, 1151–1176.
[5] C. Ha, J. H. Horner, M. Newcomb, T. R. Varick, *J. Org. Chem.* **1993**, *58*, 1194–1198.
[6] M. Newcomb, M.-H. Le Tadic-Biadatti, D. L. Chestney, E. S. Roberts, P. F. Hollenberg, *J. Am. Chem. Soc.* **1995**, *117*, 12085–12091.
[7] S.-Y. Choi, P. E. Eaton, P. F. Hollenberg, K. E. Liu, S. J. Lippard, M. Newcomb, D. A. Putt, S. P. Upadhyaya, Y. Xiong, *J. Am. Chem. Soc.* **1996**, *118*, 6547–6555.
[8] M. Newcomb, S.-Y. Choi, J. H. Horner, *J. Org. Chem.* **1999**, *64*, 1225–1231.
[9] A. M. Valentine, M.-H. Le Tadic-Biadatti, P. H. Toy, M. Newcomb, S. J. Lippard, *J. Biol. Chem.* **1999**, *274*, 10771–10776.
[10] M. L. Kemball, J. C. Walton, K. U. Ingold, *J. Chem. Soc. Perkin Trans. 2* **1982**, 1017–1023.
[11] J. Hartung, R. Stowasser, D. Vitt, G. Bringmann, *Angew. Chem.* **1996**, *108*, 3056–3059; *Angew. Chem. Int. Ed. Engl.* **1996**, *35*, 2820–2823.
[12] B. J. Maxwell, B. J. Smith, J. Tsanaktsidis, *J. Chem. Soc. Perkin Trans. 2* **2000**, 425–431.
[13] C. Chatagilialoglu, C. Ferreri, M. Lucarini, A. Venturini, A. A. Zavitsas, *Chem. Eur. J.* **1997**, *3*, 376–387.
[14] M. W. Wong, L. Radom, *J. Phys. Chem.* **1995**, *99*, 8582–8588.
[15] M. W. Wong, L. Radom, *J. Phys. Chem. A* **1998**, *102*, 2237–2245.
[16] P. M. Mayer, C. J. Parkinson, D. M. Smith, L. Radom, *J. Chem. Phys.* **1998**, *108*, 604–615.
[17] D. J. Henry, C. J. Parkinson, L. Radom, *J. Phys. Chem. A* **2002**, *106*, 7927–7936.
[18] D. M. Smith, A. Nicolaides, B. T. Golding, L. Radom, *J. Am. Chem. Soc.* **1998**, *120*, 10223–10233.
[19] A. H. Horn, T. Clark, *J. Am. Chem. Soc.* **2003**, *125*, 2809–2816.
[20] a) N. O. Brace, *J. Org. Chem.* **1967**, *32*, 2711–2717; b) D. Lal, D. Griller, S. Husband, K. U. Ingold, *J. Am. Chem. Soc.* **1974**, *96*, 6355–6357; c) P. Schmid, D. Griller, K. U. Ingold, *Int. J. Chem. Kinet.* **1979**, *11*, 333–338; d) A. L. J. Beckwith, C. J. Easton, A. K. Serelis, *J. Chem. Soc. Chem. Commun.* **1980**, 482–483.
[21] K. Vyakaranam, J. B. Barbour, J. Michl, *J. Am. Chem. Soc.* **2006**, *128*, 5610–5611.
[22] K. Vyakaranam, S. Körbe, J. Michl, *J. Am. Chem. Soc.* **2006**, *128*, 5680–5686.
[23] T. Clark, *J. Chem. Soc. Chem. Commun.* **1986**, 1774–1775.
[24] T. Clark, *J. Am. Chem. Soc.* **2006**, *128*, 11278–11285.
[25] A. Alex, E. Hänsele, T. Clark, *J. Mol. Model.* **2006**, *12*, 621–629.
[26] M. Newcomb, R. Shen, Y. Lu, M. J. Coon, P. F. Hollenberg, D. A. Kopp, S. J. Lippard, *J. Am. Chem. Soc.* **2002**, *124*, 6879–6886.
[27] K. Auclair, Z. Hu, D. M. Little, P. R. Ortiz de Montellane, J. T. Grooves, *J. Am. Chem. Soc.* **2002**, *124*, 6020–6027.
[28] C. M. Jäger, M. Hennemann, A. Mieszala, T. Clark, *J. Org. Chem.* **2008**, *73*, 1536–1545.
[29] *Electron Transfer II:* T. Clark, *Top. Curr. Chem.* **1996**, *77*.
[30] D. Kumar, S. P. de Visser, P. K. Sharma, S. Cohen, S. Shaik, *J. Am. Chem. Soc.* **2004**, *126*, 1907–1920.
[31] F. Ogliaro, N. Harris, S. Cohen, M. Filatov, S. P. de Visser, S. Shaik, *J. Am. Chem. Soc.* **2000**, *122*, 8977–8989.
[32] J. T. Groves, Y. Watanabe, *J. Am. Chem. Soc.* **1988**, *110*, 8443–8452.
[33] S. Shaik, D. Kumar, S. P. de Visser, A. Altun, W. Thiel, *Chem. Rev.* **2005**, *105*, 2279–2328.
[34] S. Shaik, H. Hirao, D. Kumar, *Nat. Prod. Rep.* **2007**, *24*, 533–552, and references therein.
[35] S. P. de Visser, D. Kumar, S. Cohen, R. Shacham, S. Shaik, *J. Am. Chem. Soc.* **2004**, *126*, 8362–8363.
[36] A. Altun, V. Guallar, R. A. Friesner, S. Shaik, W. Thiel, *J. Am. Chem. Soc.* **2006**, *128*, 3924–3925.
[37] A. Altun, S. Shaik, W. Thiel, *J. Am. Chem. Soc.* **2007**, *129*, 8978–8987.
[38] a) B. Delley, *J. Chem. Phys.* **1990**, *92*, 508–517; b) B. Delley, *J. Chem. Phys.* **2000**, *113*, 7756–7764.
[39] Materials Studio 4.2, Accelrys Inc., San Diego, **2007**.
[40] N. Govind, M. Petersen, G. Fitzgerald, D. King-Smith, J. Andzelm, *Comput. Mater. Sci.* **2003**, *28*, 250–258.
[41] H. Jónsson, G. Mills, K. W. Jacobsen, *Classical and Quantum Dynamics in Condensed Phase Simulations: Nudged Elastic Band Method for Finding Minimum Energy Paths of Transitions* (Eds.: B. J. Berne, G. Ciccotti, D. F. Coker), World Scientific, Hackensack, **1998**, p. 385.
[42] Gaussian 03, Revision C.02, M. J. Frisch, G. W. Trucks, H. B. Schlegel, G. E. Scuseria, M. A. Robb, J. R. Cheeseman, J. A. Montgomery, Jr., T. Vreven, K. N. Kudin, J. C. Burant, J. M. Millam, S. S. Iyengar, J. Tomasi, V. Barone, B. Mennucci, M. Cossi, G. Scalmani, N. Rega, G. A. Petersson, H. Nakatsuji, M. Hada, M. Ehara, K. Toyota, R. Fukuda, J. Hasegawa, M. Ishida, T. Nakajima, Y. Honda, O. Kitao, H. Nakai, M. Klene, X. Li, J. E. Knox, H. P. Hratchian, J. B. Cross, V. Bakken, C. Adamo, J. Jaramillo, R. Gomperts, R. E. Stratmann, O. Yazyev, A. J. Austin, R. Cammi, C. Pomelli, J. W. Ochterski, P. Y. Ayala, K. Morokuma, G. A. Voth, P. Salvador, J. J. Dannenberg, V. G. Zakrzewski, S. Dapprich, A. D. Daniels, M. C. Strain, O. Farkas, D. K. Malick, A. D. Rabuck, K. Raghavachari, J. B. Foresman, J. V. Ortiz, Q. Cui, A. G. Baboul, S. Clifford, J. Cioslowski, B. B. Stefanov, G. Liu, A. Liashenko, P. Piskorz, I. Komaromi, R. L. Martin, D. J. Fox, T. Keith, M. A. Al-Laham, C. Y. Peng, A. Nanayakkara, M. Challacombe, P. M. W. Gill, B. Johnson, W. Chen, M. W. Wong, C. Gonzalez, J. A. Pople, Gaussian, Inc., Pittsburgh, PA, **2003**.
[43] a) A. D. Becke, *J. Chem. Phys.* **1993**, *98*, 1372–1377; b) A. D. Becke, *J. Chem. Phys.* **1993**, *98*, 5648–5652; c) P. J. Stephens, F. J. Devlin, C. F. Chabalowski, M. J. Frisch, *J. Phys. Chem.* **1994**, *98*, 11623–11627; d) A. D. Becke, *The Challenge of d- and f-electrons: Theory and Computation* (Eds.: D. R. Salahub, M. C. Zerner), American Chemical Society, Washington, **1989**, chapter 12, pp. 165–179; e) S. H. Vosko, L. Wilk, M. Nusait, *Can. J. Phys.* **1980**, *58*, 1200–1211; f) C. Lee, W. Yang, R. G. Parr, *Phys. Rev. B* **1988**, *37*, 785–789.
[44] a) R. Ditchfield, W. J. Hehre, J. A. Pople, *J. Chem. Phys.* **1971**, *54*, 724–728; b) W. J. Hehre, R. Ditchfield, J. A. Pople, *J. Chem. Phys.* **1972**, *56*, 2257–2261; c) P. C. Hariharan, J. A. Pople, *Mol. Phys.* **1974**, *27*, 209–214; d) M. S. Gordon, *Chem. Phys. Lett.* **1980**, *76*, 163–168; e) P. C. Hariharan, J. A. Pople, *Theor. Chim. Acta* **1973**, *28*, 213–222.
[45] J. A. Pople, M. Head-Gordon, K. Raghavachari, *J. Chem. Phys.* **1987**, *87*, 5968–5975.
[46] a) G. D. Purvis, R. J. Bartlett, *J. Chem. Phys.* **1982**, *76*, 1910–1918; b) K. Raghavachari, G. W. Trucks, J. A. Pople, M. Head-Gordon, *Chem. Phys. Lett.* **1989**, *157*, 479–483.
[47] J. A. Montgomery, Jr., M. J. Frisch, J. W. Ochterski, G. A. Petersson, *J. Chem. Phys.* **1999**, *110*, 2822–2827.
[48] J. A. Montgomery, Jr., M. J. Frisch, J. W. Ochterski, G. A. Petersson, *J. Chem. Phys.* **2000**, *112*, 6532–6542.
[49] J. P. Perdew, Y. Wang, *Phys. Rev.* **1992**, *B45*, 13244–13249.
[50] P. Du, G. H. Loew, *Biophys. J.* **1995**, *68*, 69–80.

Received: June 3, 2008
Revised: November 18, 2008
Published online: January 20, 2009

